NeuroImage 83 (2013) 795–808

Contents lists available at SciVerse ScienceDirect

NeuroImage

journal homepage: www.elsevier.com/locate/ynimg

A low-frequency oscillatory neural signal in humans encodes a developing decision variable

Jan Kubanek [a,b,*], Lawrence H. Snyder [a,b], Bingni W. Brunton [c,d], Carlos D. Brody [c,d,e], Gerwin Schalk [f]

[a] Department of Anatomy and Neurobiology, Washington University School of Medicine, St. Louis, MO 63110, USA
[b] Department of Biomedical Engineering, Washington University in St. Louis, St. Louis, MO 63130, USA
[c] Princeton Neuroscience Institute, Princeton University, Princeton, NJ 08544, USA
[d] Department of Molecular Biology, Princeton University, Princeton, NJ 08544, USA
[e] Howard Hughes Medical Institute, Princeton University, Princeton, NJ 08544, USA
[f] Wadsworth Center, New York State Department of Health, Albany, NY 12201, USA

ARTICLE INFO

Article history:
Accepted 19 June 2013
Available online 18 July 2013

ABSTRACT

We often make decisions based on sensory evidence that is accumulated over a period of time. How the evidence for such decisions is represented in the brain and how such a neural representation is used to guide a subsequent action are questions of considerable interest to decision sciences. The neural correlates of developing perceptual decisions have been thoroughly investigated in the oculomotor system of macaques who communicated their decisions using an eye movement. It has been found that the evidence informing a decision to make an eye movement is in part accumulated within the same oculomotor circuits that signal the upcoming eye movement. Recent evidence suggests that the somatomotor system may exhibit an analogous property for choices made using a hand movement. To investigate this possibility, we engaged humans in a decision task in which they integrated discrete quanta of sensory information over a period of time and signaled their decision using a hand movement or an eye movement. The discrete form of the sensory evidence allowed us to infer the decision variable on which subjects base their decision on each trial and to assess the neural processes related to each quantum of the incoming decision evidence. We found that a low-frequency electrophysiological signal recorded over centroparietal regions strongly encodes the decision variable inferred in this task, and that it does so specifically for hand movement choices. The signal ramps up with a rate that is proportional to the decision variable, remains graded by the decision variable throughout the delay period, reaches a common peak shortly before a hand movement, and falls off shortly after the hand movement. Furthermore, the signal encodes the polarity of each evidence quantum, with a short latency, and retains the response level over time. Thus, this neural signal shows properties of evidence accumulation. These findings suggest that the decision-related effects observed in the oculomotor system of the monkey during eye movement choices may share the same basic properties with the decision-related effects in the somatomotor system of humans during hand movement choices.

Introduction

We often make important decisions based on sensory evidence accrued over a time period. For instance, a driver often needs to change lanes. To do so, she must carefully assess the position and speed of the neighboring vehicles. Once she has obtained enough evidence that it is safe to change lanes, she moves the steering wheel.

Pioneering work in the oculomotor system of the monkey has shed light on the neural signals that underly the fine-grained accumulation of sensory evidence and on the signals that underly the generation of the subsequent motor command. This work has revealed that neurons in oculomotor structures including the parietal eye fields (Roitman and Shadlen, 2002; Shadlen and Newsome, 1996), the frontal eye-fields (Gold and Shadlen, 2000), and the superior colliculus (Horwitz and Newsome, 1999) reflect the cumulated amount of evidence ("decision variable") on which monkeys base their decision to make an eye movement. This neural effect is observed already during the presentation of the stimulus while evidence is being accumulated. Furthermore, this work has demonstrated that the evidence for a decision to make an eye movement is represented within the same oculomotor circuits that give rise to the subsequent eye movement (Gold and Shadlen, 2000; Hanks et al., 2006).

The work in the macaque oculomotor system has laid the grounds for neurally informed theories of choice behavior (Gold and Shadlen, 2007; Ratcliff and McKoon, 2008). However, that work also raises the question whether the neural findings obtained in the macaque oculomotor systems generalize to other systems. There is some evidence

* Corresponding author at: Department of Anatomy & Neurobiology, Washington University School of Medicine, 660 S Euclid Ave, St. Louis, MO 63110, USA.
E-mail address: jan@eye-hand.wustl.edu (J. Kubanek).

1053-8119/$ – see front matter © 2013 Elsevier Inc. All rights reserved.
http://dx.doi.org/10.1016/j.neuroimage.2013.06.085

that this may be the case. In particular, recordings in monkeys have demonstrated that activity in sensorimotor regions is modulated by certain parameters of a stimulus in vibrotactile decision tasks in which a response is mediated using a hand movement (Haegens et al., 2011; Hernández et al., 2010). Furthermore, a study in humans (Donner et al., 2009) found that in a motion detection task, the centroparietal cortex shows a gradually building low-frequency signal that indicates a person's upcoming choice of which hand to use to press a button. The gradual signal buildup reported in that study is reminiscent of the signal buildup observed in the oculomotor system during an animal's plan to make a saccade into the neuronal response field (Shadlen and Newsome, 1996). As in the oculomotor system, this signal may be modulated by a decision variable (DV) on which subjects base their decision to make a given movement, and this modulation may be observed already during the presentation of the stimulus while the evidence is being accumulated. Although this possibility has been proposed (Donner et al., 2009), it has not been directly tested.

There is some evidence in recent human literature that cortical signals may be modulated by a DV (O'Connell et al., 2012; Wyart et al., 2012). The study of Wyart et al. (2012) in part shows a modulation of a low frequency cortical signal by an accumulated DV. However, this signal is modulated by the accumulated DV only shortly prior to a movement and not during the time when the evidence is being accumulated. The study of O'Connell et al. (2012) demonstrates a modulation of cortical potentials by a DV already during the accumulation period. These cortical potentials nonetheless differ from the low-frequency neural signal confined to centroparietal regions (Donner et al., 2009).

To test whether or not the centroparietal low-frequency neural signal (Donner et al., 2009) is modulated by a decision variable informing the decision to make a hand movement, we engaged humans in a perceptual decision task while recording electroencephalographic (EEG) activity. We designed a task in which the evidence for a decision is delivered to subjects in discrete quanta, through click sounds presented to the right ear and to the left ear over a brief period of time. This discrete design enables the computation of the decision variable on which a subject bases her decision on each trial, as well as the investigation of the behavior of the neural signal in regard to each quantum of the decision evidence. We found that the signal is strongly graded by the decision variable on which subjects base their decision to make a hand movement. The signal further exhibits properties of accumulation of the individual quanta of evidence.

Materials and methods

Subjects

Ten right-handed human subjects participated in the study. The subjects comprised 6 males and 4 females, aged 21 to 58. All subjects were healthy, had a normal hearing capacity, and gave informed consent through a protocol reviewed and approved by the Wadsworth Center Institutional Review Board.

Task

Subjects sat in a comfortable chair 60 cm in front of a flat-screen monitor. They wore a 16-channel EEG cap (see the Electrophysiological recordings section). Subjects wore headphones (MDR-V600, Sony) which presented a stereo auditory stimulus (see the Auditory stimulus section). The right arm rested comfortably on a pillow that was placed on a fixed table. The subjects' right hand was steadily holding a joystick (ATK 3, Logitech); subjects were ready to simultaneously press the front and top buttons of the joystick using their right index finger and the right thumb, respectively. Gaze position of each eye was measured using an eye tracker (Tobii T60, Tobii Technology) that was integrated into the flat-screen monitor. Acquisition of EEG signals, eye gaze parameters, joystick button press parameters, as well as control of the experimental design were accomplished with the BCI2000 system (Schalk and Mellinger, 2010; Schalk et al., 2004).

Each trial (see Fig. 1A) started with the presentation of a red fixation cross, 2 visual degrees in size. Subjects had to fixate at the center of the cross, and keep the eye gaze within a radius of 2 visual degrees. An absence of eye gaze within the fixation radius for more than 150 ms was considered as a break of fixation. After acquiring fixation, two icons appeared, 15° to the right and 15° to the left of the fixation cross. The right icon was a sketch of a joystick with highlighted top and front red buttons. The left icon was a sketch of the eye. At the same time, subjects were presented with a stereo auditory stimulus (click sounds, see the Auditory stimulus section), 1.0 s in duration. Subjects had to determine whether they heard more clicks in the right ear or more clicks in the left ear. The stimulus was followed by a variable delay interval, 0.3–1.3 s in duration. After the delay, the fixation cross shrank to 1° in diameter and changed its color to green. This event cued the subjects to make a movement (choice). If subjects heard more clicks in the right ear than in the left ear, they simultaneously pressed the front and the top button of the joystick using the right index finger and the right thumb, respectively. We opted for the two-finger response, as it may engage movement planning circuitry more prominently compared to if we had only used the response of a single finger response. In the analyses, movement onset was taken as the time of the earlier button press (in Figs. 2C bottom and 9, the button press is detected if either button is pressed). On the other hand, if subjects heard more clicks in the left ear than in the right ear, they made an eye movement to the left icon. If subjects broke fixation or pressed any button before the go cue, or if they failed to indicate a response within 1200 ms after the go cue, the trial was aborted and excluded from the analyses. A trial was also aborted if subjects responded with both movements. The type of error was indicated to the subjects in red, large-font text (TOO EARLY, TOO LATE, MOVED BOTH). A successful choice was communicated to the subject by shrinking the icon corresponding to the chosen movement (the eye icon or the joystick icon) from 2° in size to 1° in size. After subjects re-acquired fixation and released all buttons, they were given feedback, 0.6 s in duration, indicating whether they were correct or not. A correct response was indicated by a green text (+10c, +20c, +30c, +40c, or +50c; in the order of increasing stimulus difficulty). An incorrect response was indicated by a red text (−50c, −40c, −30c, −20c, or −10c). The offset of feedback was followed by a variable inter-trial interval, 0.6–1.2 s in duration.

Auditory stimulus

The auditory stimulus presented to each ear consisted of a train of brief (0.2 ms) click sounds drawn from a homogeneous Poisson process. Each train lasted 1.0 s. The stereo stimulus was composed such that the sum of clicks presented to the left ear (C_l) plus the sum of clicks presented to the right ear (C_r) summed to a fixed number $C_l + C_r = \Omega$, $\Omega \in \{25,32,39,46\}$. The value of Ω was drawn randomly on each trial. We imposed the Ω randomization to ensure that subject had to pay attention to the click sounds in both ears. Stimulus presentation was also subject to the constraint that two consecutive clicks had to be separated by at least 5 ms. Furthermore, during early tests of the paradigm, subjects often claimed that they were biased toward the ear that presented either the first or the last click. To avoid such possible bias, the first and the last clicks in each stimulus occurred in both ears simultaneously, at time 0.0 s and 1.0 s, respectively. Thus, each ear heard at least 2 clicks, and at most $\Omega - 2$ clicks. We generated ten random versions of all the 130 possible combinations of C_l and C_r, and loaded the corresponding files into the memory of the BCI2000 system prior to the start of each experiment.

Behavioral model

We inferred the variable on which subjects base their decision ("decision variable") using a behavioral model. The model takes the number of clicks presented to the right ear C_r and to the left ear C_l in

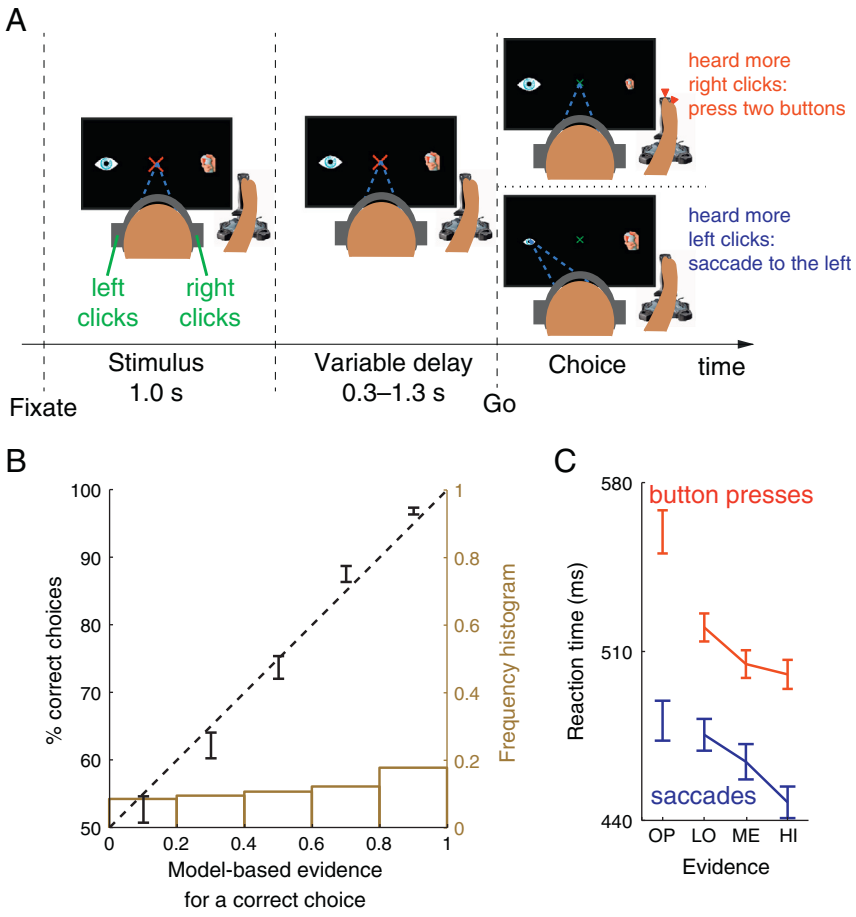

Fig. 1. Decision task and behavioral model. (A) After acquiring a fixation cross, subjects listen to a binaurally presented auditory stimulus. Subjects decide whether they hear more click sounds in the right ear or in the left ear. The stimulus is followed by a variable delay period. After the delay, the fixation cross shrinks and changes color to green, thus cuing the subject to make a choice. If subjects heard more clicks in the right ear, they press two buttons of the joystick with their right index finger and the thumb. Otherwise, they make a saccade to an eye icon on the left side of the screen. (B) Mean ± SEM percentage of subjects' correct choices as a function of the modeled evidence for that response. The dashed line represents an ideal match between the model's predictions and the probabilistic behavior. The ideal match explains 97.6% of the variance in the 5 data points. The brown histogram gives the number of trials in each bin. (C) Mean ± SEM reaction time for four levels of decision evidence (see text), separately for button press choices (red), and saccade choices (blue).

each trial as its inputs, and returns the evidence E_r for the rightward choice:

$$E_r = \frac{2}{1 + \exp\left(-\beta \frac{C_r - C_l}{C_r + C_l}\right)} - 1.$$

If $E_r = 1$, the evidence for the rightward choice is maximal; if $E_r = 0$, no evidence can be gathered; if $E_r = -1$, the evidence is maximal for the leftward choice. The numerator of the expression $\frac{C_r - C_l}{C_r + C_l}$ compares C_r and C_l. The denominator accounts for the "distance effect" (Moyer and Bayer, 1976)—it is easier to distinguish between C_r and C_l when they are small compared to when they are large. The inverse temperature parameter β is a parameter of the sigmoid transformation. It is a marker of psychophysical performance—β grows with growing ability to distinguish the left and the right stimulus.

We fitted the model's parameters to account for each subject's choices. We found that subjects were biased toward choosing the rightward option—they chose the rightward option in 55% of cases. To account for this bias, we included in the model a bias term B:

$$E_r = \frac{2}{1 + exp\left(-\beta\left(\frac{C_r - C_l}{C_r + C_l} + B\right)\right)} - 1. \quad (1)$$

The two free parameters β and B were fitted to the choice data of each session according to the maximum likelihood procedure—maximizing the log likelihood criterion (L):

$$L = \sum_t \ln\left(E_r(t) r(t)\right),$$

where the variable $r(t)$ equals to + 1 if the subject on trial t chose the rightward option, otherwise equals − 1. The fit resulted, over the 10 subjects, in $\beta = 6.9 \pm 2.4$ (mean ± SD), and in $B = +0.060 \pm 0.070$.

Decision evidence and click step at each time point

The value of the decision variable (decision evidence) at time t (Figs. 7 and 8) is

$$E_r(t) = \frac{2}{1 + \exp\left(-\beta\left(\frac{\int_0^t [c_r(\tau) - c_l(\tau)] d\tau}{\int_0^t [c_r(\tau) + c_l(\tau)] d\tau} + B\right)\right)} - 1,$$

where $\int_0^t c_r(\tau)$ and $\int_0^t c_l(\tau)$ are the numbers of right and left clicks, respectively, presented up to time t. The parameters β and B are estimated as above, i.e., after all evidence has been presented.

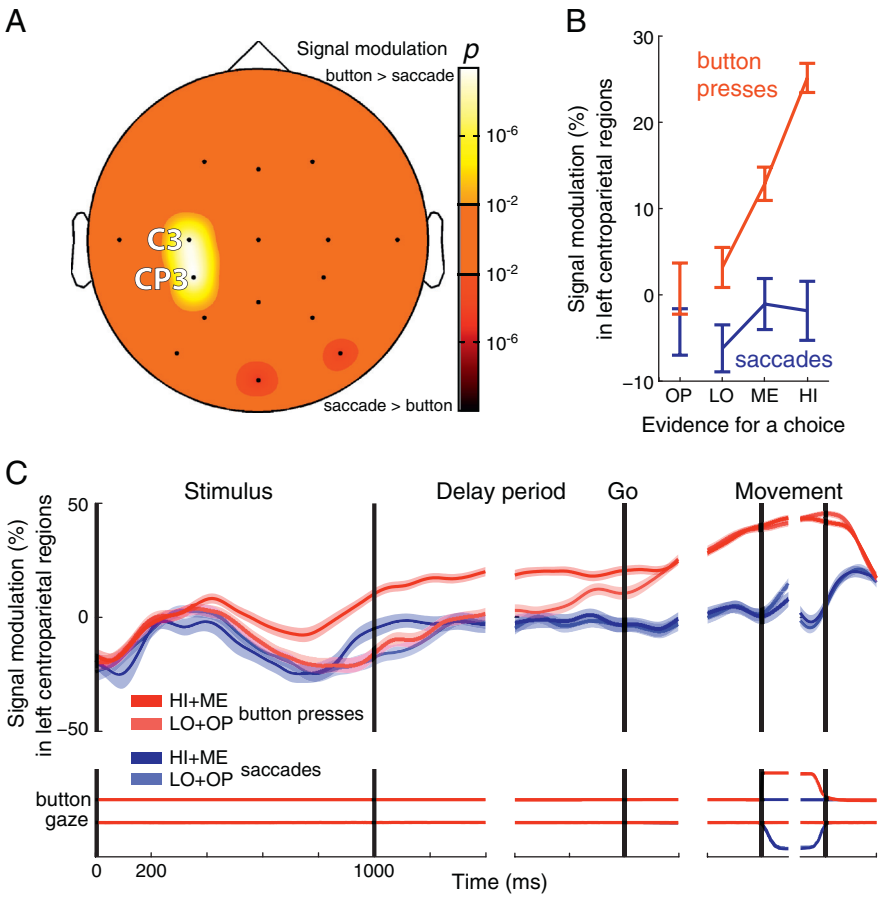

Fig. 2. The human centroparietal cortex reflects the dynamics of a perceptual decision process. (A) Topography of the choice effect, i.e., the significance of the difference between desynchronization on button press versus saccade trials during the delay period. The bright colors represent locations at which neural activity is more desynchronized for button presses compared to saccades. The dark colors represent the converse. (B) Mean ± SEM neural desynchronization at C3 and CP3 during the delay period as a function of decision evidence, separately for button press choices (red), and saccade choices (blue). (C) Mean ± SEM desynchronization at C3 and CP3 as a function of time. Data are shown separately for button press choices (red) and saccade choices (blue), and choices for which evidence was either strong (dark) or weak (light)—see inset. Desynchronization was measured in 100 ms periods overlapping by 1 sample (3.9 ms). The bottom part of the plot shows the mean ± SEM button press and eye gaze signals, respectively.

In the analysis shown in Fig. 8, we further defined a "click step" signal $in(t)$ that conveys the temporal progression of the input, the individual click elements. For a given trial, this signal equals $+1$ (-1) at the time a right (left) click is presented, and retains this value until the next click is presented. Mathematically, the value of this input signal at time t is

$$in(t) = \sum_i s_i \left[H(t-t_i) - H(t-t_{i+1})\right],$$

where t_i is the time of the occurrence of the i-th click, $H(t)$ is the Heaviside step function, and $s_i = +1$ if the i-th click is a right click and $s_i = -1$ if the i-th click is a left click.

Online adaptive procedure

Our objective was to make our subjects at times certain and at times uncertain about their decision, with a uniform spectrum in between. To achieve that, E_r was drawn in each trial from a uniform distribution over the interval $(-1, +1)$. Having generated a random E_r, we then randomly selected one of the 10 pre-generated auditory stimuli with such C_r and C_l that—according to the current model—most closely correspond to the generated E_r. From Eq. (1), it follows that

$$C_r = \left(\frac{1}{2\beta} \ln\left(\frac{E_r}{1-E_r}\right) + \frac{1}{2}\right)\Omega, \qquad (2)$$

where $\Omega = C_r + C_l$ and thus $C_l = \Omega - C_r$. To keep the online adaptation task one-dimensional (optimizing one parameter β only), the online procedure did not include the choice bias term (we set $B = 0$ in Eq. (1) during the online procedure, and thus Eq. (2) does not feature this term).

We designed the experiment to adjust the difficulty of the presented stimuli to the performance of each subject. Our objective was to keep each subject at approximately 75% correct responses. To achieve this, an online algorithm adapted the value of β (initial value in Eq. (2), $\beta = 4$) to each subject's performance over the last 20 trials according to the following update rule:

$$\beta_{\text{new}} = \beta_{\text{old}} 1.2^{(A-75)/10},$$

where A is the accuracy, in %, over the past 20 trials. Notice that when $A > 75$, β increases; when $A < 75$, β decreases; and when $A = 75$, β does not change. This procedure allowed subjects to perform close to the desired accuracy (75.4% ± 2.0% (mean ± SD)).

Each session started with a sequence of 10 easy warm-up stimuli $(E = [+1, -1, +1, -1, -1, +1, +1, -1, +1, -1])$ (these values are approximate to the actually presented evidence because each stimulus contained at least two clicks and thus E must always fall slightly short of ± 1)). If a subject reached at least 75% accuracy during this warm-up, the adaptive procedure was initiated. Otherwise, the warm-up was extended by another 10 trials. Only one subject needed an additional 10 warm-up trials to reach the 75% accuracy.

Electrophysiological recordings

Neural data were recorded using a 16-channel EEG cap (Electro-Cap International, Inc., Eaton, OH). The channels were positioned according to the International 10–20 method of electrode placement (F3, Fz, F4, T7, C3, Cz, C4, T8, CP3, CP4, P3, Pz, P4, PO7, PO8, Oz). The left and right mastoids served as ground and reference, respectively. The neural signals were acquired with a g.USBamp series B amplifier (g.tec, Graz, Austria) at 24-bit resolution at a rate of 256 Hz per channel. The device applied appropriate antialiasing filters.

Signal processing

The acquired neural data were filtered using an IIR filter in the alpha and beta frequency range (8–26 Hz; 80 dB cut-off at 7 Hz and 30 Hz). To avoid phase distortion, we applied the filter using the filtfilt() function in Matlab (The MathWorks, Natick, MA). This filtering method performed zero-phase digital filtering by processing the input data in both the forward and reverse directions. The signals were then re-referenced to a common reference: for a given channel, the voltage waveform resulting from averaging the voltage waveforms over all channels was subtracted from the voltage waveform at that given channel. For each channel, we computed "desynchronization" as the relative decrease in power of the filtered signals in a particular temporal window of interest with respect to the mean power at that channel over the entire session of each subject. Although desynchronization could be computed relative to a baseline preceding each trial, we did not have to resort to such additional manipulation to obtain robust effects.

Visualization of evidence

Throughout the paper, we quantified behavioral and neural effects over individual trials (trial-wise analysis). To present data graphically, we grouped the data for a given correct choice into three terciles of growing evidence for that choice (LO, ME, HI). In addition, we also assessed the cases in which evidence points in the opposite direction with respect to a given choice ($E < 0$; OP). From the perspective of the experimenter, the OP trials represent error (incorrect choice) trials. From the perspective of the subject (when the subject's choice is ignored), OP trials are of the same kind as the correct trials.

Visualization of topographies

We visualized data at each channel using the topoplot function available at http://sccn.ucsd.edu/eeglab/allfunctions/topoplot.html.

Statistical analysis

We test the significance of an effect using the general linear ANOVA or ANCOVA models. These models feature the variable being tested (e.g., a variable indicating whether a subject chose a button press or a saccade) and include subject as an additional random group variable. When performing the analysis in Fig. 2A, we excluded from the concatenated data the top and the bottom 1% of desynchronization values. The removal of the outliers increased the statistical robustness of the effect reported in this figure. In subsequent analyses, all data were included. All topographical plots were Bonferroni corrected for the number of channels (by the factor of 16 in Fig. 2A), and for the number of channels and comparisons (by the factor of $16 * 2$ in Fig. 9).

Trial-wise fits to neural data during the stimulus period

We tested whether neural data on each trial during the stimulus period are better approximated with a line function or a step function. A line has two free parameters—slope S and intercept I. A step has three free parameters—starting level L_s, time of the step T, and ending level L_e. The step fit was allowed to be flat (at a constant value L_s). We asked which of these two fits explains more variance in the neural data on each trial. To compare these two fits in a fair way, we reduced the number of free parameters such that each fit had one free parameter (line: S, step: T). We did this in two ways. First, we set $L_e = 33.0$, which is the level of average neural signal at the end of the stimulus period for high evidence trials. We chose the high evidence level, because the step function shall emulate a binary change of state from uncertain (about which option to choose) to certain. On average, subjects are likely more certain at the end of the stimulus presentation during high evidence trials compared to trials in which evidence was low. Second, before computing the fits, we subtracted from neural activity on each trial the baseline neural activity on that trial. We defined the baseline as the average neural activity on each trial in the interval 0 to 200 ms following the onset of the stimulus. By subtracting away the baseline, we reduced the number of free parameters of each fit by one (we spared the use of the I parameter of the line, and the L_s parameter of the step). This way, both fits had 1 free parameter (S and T for the line and step fits, respectively). We then measured the proportion of variance that each fit (f) explains in the neural signal (s): $R^2 = 1 - \frac{\mathrm{Var}(s-f)}{\mathrm{Var}(s)}$. Notice that if a fit f is grossly inadequate, $\mathrm{Var}(s - f) > \mathrm{Var}(s)$, and thus it is possible for R^2 to be negative. We validated this procedure using an additional simulation. This simulation amplitude-modulated a 10 Hz signal by a step function, subsequently performed the same filtering/fitting functions as described above, and correctly identified that the step function was a better fit to the data than the line function.

The above analysis uses a heuristic to match the number of parameters in the two models. We also performed an analysis that did not constrain the two models. In particular, the Bayesian information criterion (BIC; Schwarz, 1978) evaluates the likelihood of a model candidate to be suitable to account for the data while penalizing the number of free parameters. This information criterion is computed as $\mathrm{BIC} = n \ln(\sigma_e^2) + k \ln(n)$ where n is the number of samples (in our case, 256 samples during the 1.0 s stimulus period), k is the number of parameters to be estimated ($k = 2$ for the line fit, $k = 3$ for the step fit), and σ_e^2 is the variance in the error residuals, $\sigma_e^2 = \frac{1}{n}\sum_{i=1}^{n}(x_i - \hat{x}_i)^2$ where x_i are the actual samples and x_i are the samples estimated by the model fit. Note that a caveat of this method over the above heuristic method is that the BIC computation assumes independence of the individual samples. It is however unclear at which sampling rate should the individual samples of a neural signal, if at all, be considered independent. This analysis, in comparison to the heuristic method, should thus be interpreted with care.

Accounting for eye gaze and reaction time

We tested whether the neural effects can be explained, besides decision evidence E, by eye gaze parameters or the subject's reaction time. Specifically, we quantified, during the delay period, and during movement, the mean horizontal gaze position (G_{mean}), the variance in horizontal gaze position (G_{var}) and the subject's reaction time (RT). These variables were considered as additional regressors, besides E, in the multiple regression on neural activity on each trial:

$$\mathrm{Desyn} = \mathrm{Slope}E + \beta_1 G_{\mathrm{mean}} + \beta_2 G_{\mathrm{var}} + \beta_3 RT + \gamma, \quad (3)$$

where Desyn is the amplitude of desychronization as described above, E is the decision evidence (Eq. (1)), and Slope, β_i, and γ are the coefficients to be determined.

Measurement of hand EMG

We measured the electromyographic (EMG) activity of the anterior forearm muscles in ten subjects in a modified version of the task that used the same stimuli and the same stimulus period. Bipolar measurements were made through two surface leads (GS27 pre-gelled disposable

sEMG sensors) placed 2 cm apart along the flexor carpi radialis, and two surface leads placed 2 cm apart along the flexor digitorum superficialis (which may in part also reflect activity of the palmaris longus). For both muscles, we used the lead further apart from the wrist as the recording reference. The EMG signals were filtered using an IIR band-pass filter (20–100 Hz, 80 dB cut-off at 19 Hz and 105 Hz). To avoid phase distortion, we applied the filter using the filtfilt() function in Matlab. The EMG power was measured in 100 ms windows overlapping by 1 sample (3.9 ms).

Results

Decision task

We engaged humans in a perceptual decision task (B.W.B. and C.D.B., *Soc. for Neurosci.* No. 281.7 (2009); Brunton et al., 2013). In this task, subjects listen to a stereo auditory stimulus comprising a 1.0 s train of Poisson-distributed click sounds (see the Materials and methods section). Subjects decide whether they hear more clicks in the right ear or more clicks in the left ear. We used this task over alternatives (e.g., the dot motion stimulus initially used to compare psychometric to neurometric discrimination performance in the motion-sensitive area MT (Britten et al., 1992)), as in this task the individual quanta of evidence for and against a decision are well defined and separated in time. These discrete elements of decision evidence allow us to construct a simple analytic model of subjects' choice behavior. Furthermore, this task allows us to investigate the neural encoding of each element of the decision evidence.

To indicate that subjects heard more clicks in the right ear, they press the top and the front buttons of a joystick with their right index finger and the thumb (see the Materials and methods section). To indicate that subjects heard more clicks in the left ear, they make a saccade to a target on their left (Fig. 1A). The stimulus is followed by a variable delay interval (300 ms–1300 ms). After the delay, a go cue signals subjects to make a choice. We introduced the variable delay for two reasons. First, the delay period is an ideal portion of the trial to quantify the neural effect, as in this period data are not confounded by sensory parameters of the stimulus (since all evidence has been already presented) or by subsequent elements of the task (e.g., the go cue). Second, the variable nature of the delay prevents subjects from anticipating the go cue and thus from planning a response before they are cued to do so. This is to eliminate the possible purely motor confounds. A choice was considered valid if it came within 1200 ms after the presentation of the go cue. Trials with premature or late choices were aborted and discarded.

Behavior

Subjects learned the task rapidly, in most cases within the first 10 warm-up trials (see the Materials and methods section). The percentage of valid choices was 93.4% ± 3.1% (mean ± SD) across the 10 subjects. Each of the 10 subjects completed two sessions, and each session consisted of 200 valid trials. An algorithm monitored subject performance on-line and adjusted task difficulty so as to keep performance levels close to 75% correct (see the Materials and methods section).

Behavioral model

To estimate the decision variable (DV) on which subjects base their decision, we fit each subject's behavior using a behavioral model. The model compares the sum of the clicks accumulated in the right ear to the sum of the clicks accumulated in the left ear, and passes the result through a sigmoid function to give the resulting DV (see the Materials and methods section). We validated the model by observing a close match between the modeled DV and the actual behavior (Fig. 1B). The figure shows that the modeled DV serves as an estimate of the amount of subjective evidence (briefly, "evidence") a subject has obtained for a response: the more evidence was cumulated in favor of a response, the more likely a subject is to choose that response.

Fig. 1B, brown histogram, shows that subjects were presented with trials of low evidence and with trials of high evidence, with a continuum in between. This was the goal of our experimental design. The slightly higher proportion of trials in which evidence is high is due to the convergence time of the online adaptive procedure—the procedure started with easy trials before it adapted to each subject's performance (see the Materials and methods section).

When a subject has obtained strong evidence for a decision, she may respond faster. The model's output may therefore reflect not only subjective evidence but also reaction time. This is indeed what we found (Fig. 1C). In this and following figures, decision evidence was discretized (see the Materials and methods section) such that the first bin (OP) refers to evidence pointing in the opposite direction to a given choice (error trials from the perspective of the experimenter), and LO, ME, and HI refer to correct choices of growing evidence for those choices. In this and following analyses, we quantify behavioral and neural effects over individual trials (trial-wise analysis), and include all trials, i.e., trials spanning the full range of decision evidence, in the analysis. The slope of evidence on RT in an ANCOVA model (see the Materials and methods section) is − 33.8 ms ($p = 0.017$, $F_{1,1774} = 5.7$) for saccades and − 100.3 ms ($p < 10^{-11}$, $F_{1,2209} = 50.7$) for button presses. The decrease remains significant when only correct choices are considered ($p < 10^{-3}$, $F_{1,1260} = 12.1$, and $p < 10^{-3}$, $F_{1,1839} = 11.6$ for saccades and button presses, respectively). The presence of this effect is of independent interest given that subjects had ample time to make up their mind during the presentation of the stimulus (1.0 s) and the delay period (0.8 s on average).

An electrophysiological signal encodes choice

It has been shown that low-frequency cortical signals recorded over centroparietal regions encode an upcoming choice of a hand movement (Donner et al., 2009). We first tested whether our data reproduce this finding. To do so, we band-pass filtered the recorded neural signals in a range spanning the alpha-beta portion of the spectrum (8–26 Hz, see the Materials and methods section for details). For a given session and channel, we then computed the change in power ("desynchronization") of the filtered signals during the delay period—while subjects were holding a decision in their memory—relative to the mean power for that channel over the entire session. We then assessed the effect of *choice* (also referred to in this paper as *decision outcome*, *motor command*, *motor plan*, or *action*) by contrasting neural activity on trials in which subjects chose the button press with neural activity on trials in which subjects chose the saccade.

Fig. 2A shows the spatial extent of the neural effect of decision outcome (choice of a saccade or a button press) during the delay period. The figure reveals a highly significant and localized difference in neural activity for the two movement plans. Specifically, plans to make a button press are accompanied by a substantially higher desynchronization compared to plans to make a saccade. The effect peaks at channels C3 (ANOVA, $p < 10^{-9}$, $F_{1,3846} = 44.2$) and CP3 ($p < 10^{-9}$, $F_{1,3846} = 41.6$), which are positioned over the centroparietal cortex contralateral to the involved hand. Since C3 and CP3 show similar effects, we henceforth average neural activity over these two channels.

The neural signal encodes the input decision variable

To test the central hypothesis of this study, we then investigated whether the same neural signal encodes the input variable on which a decision is based (i.e., the inferred DV, "decision evidence"). Specifically, we tested whether for a given decision outcome—for a single, fixed movement—the signal is modulated by the decision evidence for that movement.

We found that the signal is strongly modulated by decision evidence (Fig. 2B). For all trials that resulted in a button press (red), neural activity during the delay period is desynchronized in a graded fashion as a function of growing evidence. The magnitude of this modulation (slope of desynchronization over decision evidence; ANCOVA) is 30.2% ($p < 10^{-9}$, $F_{1,2182} = 40.2$). The effect is weaker for trials that resulted into a saccade (blue), with a modulation of 12.6% ($p = 0.022$, $F_{1,1713} = 5.2$). Similar results are obtained when we split the data by individual subject: the signal encodes the decision variable in the 10 subjects during button press choices (median slope 22.7%, $p = 0.002$, two-tailed Wilcoxon signed rank test, $N = 10$), and less prominently during saccade choices (median slope 8.7%, $p = 0.084$, two-tailed Wilcoxon signed rank test, $N = 10$).

Dynamics of the neural signal

We then investigated the time course of the decision- and choice-related effects. Fig. 2C presents the signal as a function of time separately for button press (red) and saccade (blue) choices, and separately for choices for which evidence was strong (dark) and for which evidence was weak (light). Thus, the figure shows two effects—the effect of decision evidence (dark versus light) and the effect of decision outcome (red versus blue). First, we focus on the effect of decision evidence, for all button press trials (dark red versus light red). A significant difference between the two traces is observed starting at 481 ms following stimulus onset (Wilcoxon rank sum test, $p < 0.05$ for at least ten consecutive time samples). The magnitude of the difference grows throughout the stimulus period, remains steady during the delay period, weakens toward the end of the delay period, and disappears entirely shortly after the go cue. Second, we focus on the effect of decision outcome (red versus blue). Button press choices (red), compared to saccades (blue), are accompanied by a substantial desynchronization of the centroparietal rhythms. Desynchronization for button press choices continues to grow from the time of the go cue, and falls off sharply immediately after the movement. Notably, at the time of the movement, the signal reaches a common level irrespective of the amount of evidence that has accumulated for the decision to make a button press. Such signal property may be an indicator of a presence of a choice bound, one of the defining properties of the diffusion-to-bound class of models of choice behavior in reaction-time (Stone, 1960; Edwards, 1965; Vickers, 1970; Gold and Shadlen, 2007). This possibility should specifically be tested in reaction time tasks in the future.

The signal is graded by the decision variable early in the trial

Fig. 2C reveals that for button press choices, the difference in the signal during high evidence and low evidence stimuli increases throughout the stimulus period. This effect is obscured by the low-frequency transient that occurs from about 0.2 s to 0.6 s after stimulus onset and is common to all trials. As a control, we subtracted the mean saccade trace from each button press trace. The result is shown in Fig. 3. The figure reveals that the strength of desynchronization ramps upward or downward with a rate that increases with the amount of sensory evidence—the more evidence, the faster (steeper) the rise. The rise stops around the time of the offset of the stimulus. Following stimulus offset, the effect drops off slightly, yet the signal remains substantially graded by the strength of decision evidence throughout the delay period. The signal reaches a common level at the time of the behavioral response, and falls off sharply thereafter.

To confirm that the signal during the stimulus period builds up with a rate that is proportional to decision evidence, we fitted a line to the neural signal on each trial during the stimulus period, and measured the slope of this line fit as a function of decision evidence. Indeed, the slopes of the trial-wise line fits are steeper with increasing decision evidence (Fig. 4) and this effect is significant (ANCOVA, $p < 10^{-4}$, $F_{1,1828} = 19.3$).

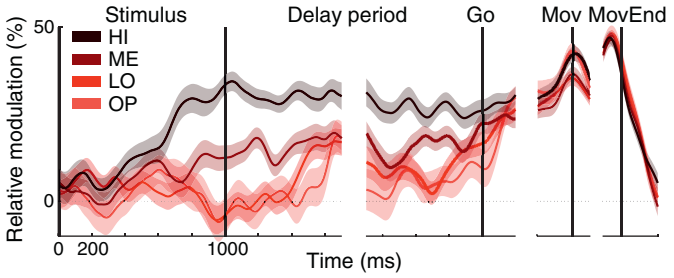

Fig. 3. Signal dynamics during hand-movement choices. Mean ± SEM button press desynchronization for four levels of evidence (HI, ME, LO, OP) relative to the average desynchronization for all saccade trials.

The average signals observed in Fig. 3 diverge continuously throughout the stimulus period. It is possible that this continuous trend could be produced by averaging, across trials, a truly continuous signal (such as the considered line function), or else by an abrupt motor switch signal (a step function) that on each trial changes its state from low to high at varying times distributed over the stimulus period. There is, however, no increase in trial-by-trial variance during the period in which the signal rises, compared to the periods immediately before and after this rise. This argues against a series of abrupt steps distributed in time. To further distinguish between these two possibilities, we fitted two functions to the neural (Fig. 3) on each trial during the stimulus period—a line, and a step function. As in Fig. 3, in this analysis, the mean neural signal during saccade choices was subtracted from the neural signal on each trial during button press choices. The step fit was allowed to remain flat, i.e., not to ramp at all. We then asked which of these two fits was a better approximation of the neural data (see the Materials and methods section and Fig. 5A). Although both fits have one free parameter, the trial-wise line fit explains substantially more variance (mean $R^2 = 0.16$) than the trial-wise step fit (mean $R^2 = 0.08$), and this difference is significant (ANOVA, $p < 10^{-4}$, $F_{1,1809} = 18.9$).

We further compared the two fits using the Bayesian information criterion (BIC; Schwarz, 1978). The BIC evaluates the likelihood of a model candidate to be suitable to account for data while penalizing model's complexity (the number of free parameters to be estimated). The penalty for the number of parameters bypasses the necessity to match the number of parameters in each model. The unconstrained models have two (line fit) and three (step fit) parameters (see the Materials and methods section). Fig. 5B gives the BIC for each of the

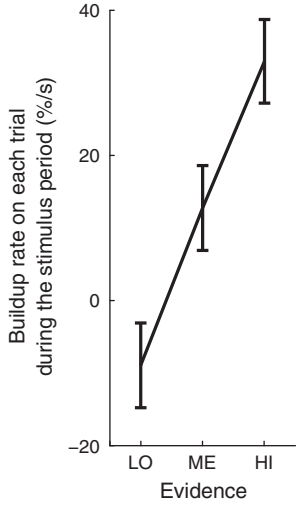

Fig. 4. The steepness of the early ramping activity on each trial is proportional to decision evidence. Rate of rise (slope) of linear fits to the neural signal during the stimulus period, computed on each trial. These trial-wise slopes are binned according to increasing decision evidence. The error bars represent the SEM.

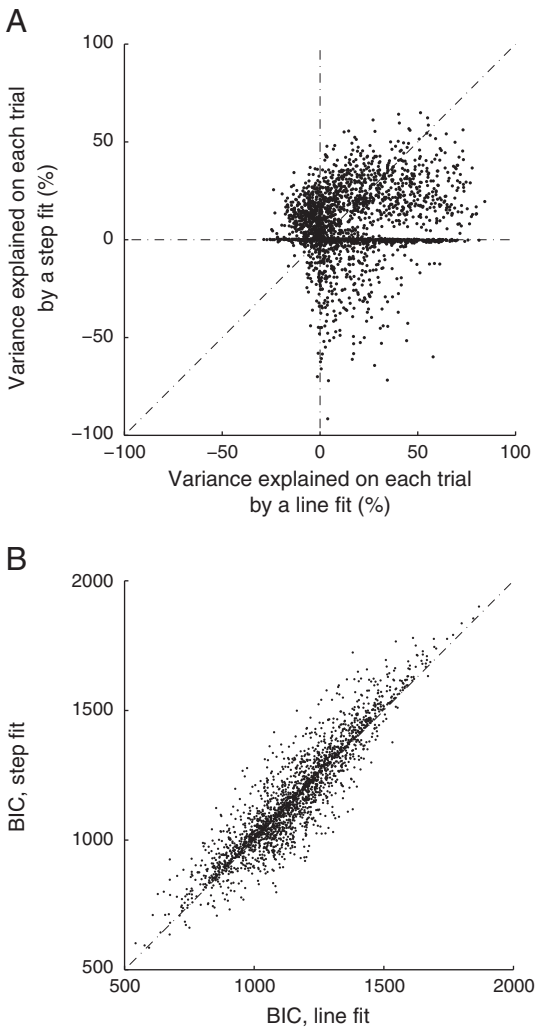

Fig. 5. Line fit explains the early ramping activity during the stimulus period on each trial better than a step fit. (A) Variance explained on each trial in the neural signal during the stimulus period. The figure compares, for each trial, the variance explained by a line fit (abscissa) versus variance explained by a step fit (ordinate)—see text for details. The line fit explains substantially more variance (mean $R^2 = 0.16$) than the trial-wise step fit (mean $R^2 = 0.08$). (B) The Bayesian information criterion (BIC) computed for the same data as in A. The line fit model is associated with a significantly smaller BIC (see text), and thus represents a better fit to the data than the step fit model.

two models, for each button press trial. The line fit gives the mean BIC of 1151.2, the step fit 1162.6 (mean difference of 11.4). This difference is substantial and corresponds to the probability ratio of 305.6 : 1 (Eq. (22) in Raftery, 1995) that the line fit is the better fitting model (a lower BIC indicates a better candidate).

The results of these analyses suggest that the ramping signal observed in the average time courses in Fig. 3 is also present during individual trials.

The signal shows properties of early evidence accumulation

Thus far, we demonstrated that the neural signal is modulated by a decision variable that quantifies the amount of evidence accrued for a decision during the stimulus period. Furthermore, we have shown that the buildup rate of the signal during the stimulus period is governed by the amount of the accumulated evidence. This raises the possibility that the neural signal may in part encode the cumulative sum of the individual quanta of evidence, an integral of the sort featured in drift-diffusion models of choice behavior in reaction-time tasks (Edwards, 1965; Ratcliff and McKoon, 2008; Stone, 1960; Vickers, 1970).

A signal that represents an integral of the individual quanta of evidence must exhibit three crucial properties. First, the signal must respond rapidly to each incoming quantum of evidence (the click sound in our case). Second, that response must distinguish the quantum of evidence that supports a given decision from the quantum that speaks against that decision (in our case, a right click informing the decision to make a button press from a left click contradicting that decision). Third, the response must show a memory trace, i.e., a sign of temporal integration; the response must not be transient in nature.

We tested whether the signal reported in our study shows these three properties. The design of our task allows us to test these properties without the necessity to assume a particular behavioral model. Specifically, we investigated the behavior of the signal in regard to each evidence element by aligning the signal to the onset time of each click. The responses to the right and the left click, relatively to average response to all clicks, for all trials that result in a button press, are given in Fig. 6. Fig. 6 top left gives the responses in the left centroparietal regions and includes clicks from the entire stimulus interval. The figure reveals that the signal strongly distinguishes the evidence in support of a button press (a right click) from the contrary evidence (a left click). The response to a click is robust and rapid; a significant difference between a right and a left click is observed starting at 74 ms ($p < 0.01$, two-tailed t-test) following a click. Following the initial response, the distinction between the right and the left click responses remains significant throughout the trial. Note that the maintained difference is not due to the occurrence of clicks following the current click of interest, because in that case the signal would show the same difference for clicks *preceding* the current click; no significant difference between the responses is observed prior to a click.

Importantly, these responses are unlikely to represent purely sensory responses, for two reasons. First, the effect shows a steady temporal, not a transient characteristic. Second and critically, the effect is not observed over auditory regions of the same hemisphere (channel T7; Fig. 6 bottom left).

We further investigated whether the signal shows the properties of evidence accumulation already early in the trial, for clicks occurring within the first 400 ms. This investigation is important given that the signal is impacted by a transient common to all data early in the trial (Fig. 2C). Indeed, while the effect is reduced in magnitude, we observe the same principal characteristics in this early portion of the trial (Fig. 6 right panels).

Together, the signal reported in our study shows rapid, evidence-polarity-specific, and maintained responses to each quantum of decision evidence.

Encoding of the decision variable at each time during integration

If the neural signal reported in this study in part encodes an integral of each decision quantum, the signal should encode the instantaneous value of the decision evidence at each time during the evidence accumulation. We tested this possibility by computing the correlation of the instantaneous value of the decision variable at a given time during the evidence accumulation (see the Materials and methods section) and the instantaneous value of the neural signal at that time. The result, for all trials that result in a button press, is given in Fig. 7.

The figure reveals that the neural signal encodes the instantaneous value of the evidence that has accumulated for a decision at each time throughout the stimulus period. The effect reaches significance already early during the stimulus period, starting at 137 ms following stimulus onset. In line with the result of Fig. 6, the correlation of the neural signal with the decision evidence rises progressively throughout the stimulus period and reaches a maximum at the end of the stimulus period. This effect likely reflects a property of the neural circuitry given that a behavioral study using a large data set found that subjects assign approximately equal weight to clicks occurring at different times throughout the stimulus period (Brunton et al., 2013).

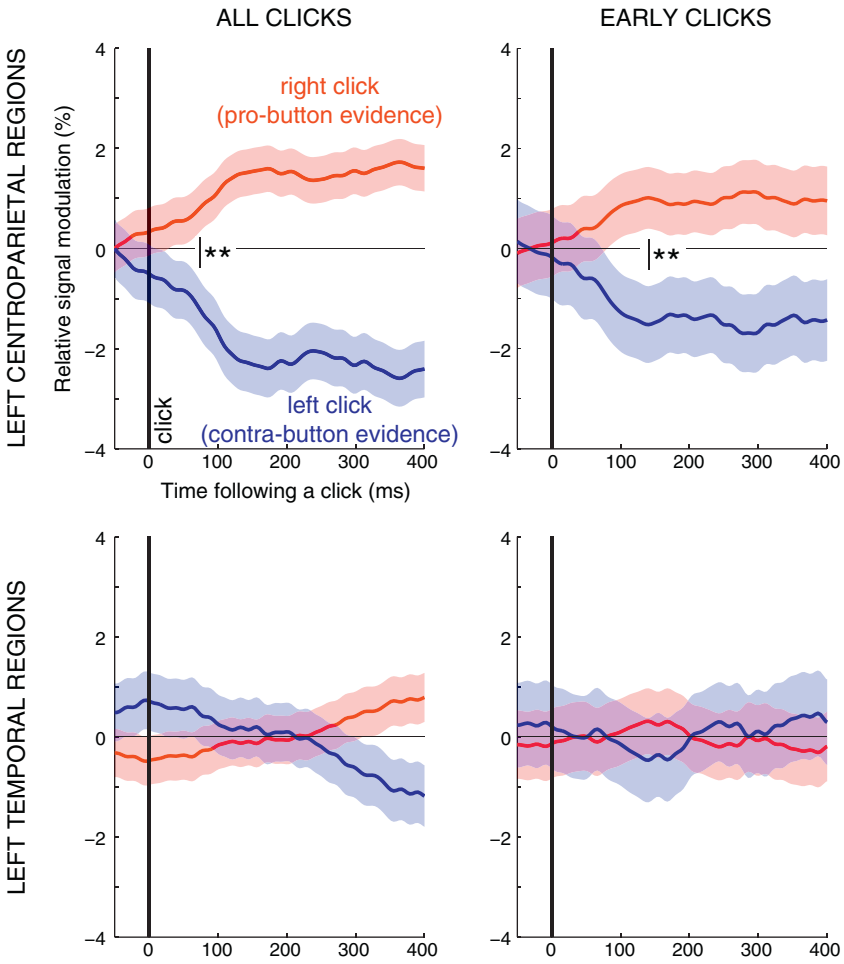

Fig. 6. The neural signal encodes the polarity of each element of decision evidence. Each trace gives the mean ± SEM change of the neural signal following a right click (red) and a left click (blue), relative to average response to all clicks, for all trials that result in a button-press. The top panels give the responses in the left centroparietal regions considered previously in the paper (channels C3 and CP3). The bottom panels give the responses in the left temporal regions (channel T7). The left panels include all clicks during the stimulus period. The right panels include clicks that occur within the first 400 ms of the stimulus period. The thick vertical line at time 0 marks the occurrence of a click. The thin vertical line with the two stars indicates the time when the red and blue curves start to significantly differ ($p < 0.01$, two-tailed t-test). As elsewhere in the paper, the desynchronization of the neural signal was measured in 100 ms windows, 1 sample (3.9 ms) overlap.

Comparison of the encoding of the input quanta and the cumulated decision evidence

The neural signal encodes the polarity of each evidence quantum (Fig. 6), as well as the instantaneous cumulated evidence (Fig. 7). Next, we directly compared the encoding of these two quantities. We aligned the data to the onset of each click. We then regressed the instantaneous cumulated evidence (the quantity used in the previous paragraph) and a signal that represents the onset and the polarity of each click ("click step", see the Materials and methods section) on the neural signal, separately for each time point following a click. We then assessed the t-statistic of the associated weights in this linear model, at each time point following a click (Fig. 8).

The figure shows that the input evidence elements and the cumulated evidence significantly contribute to the variability in the neural signal. The figure reveals that the cumulated evidence is encoded much more strongly compared to the input evidence elements (mean t over the 300 ms following a click: $t_{\text{evidence}} = 14.1$, $t_{\text{input}} = 4.8$). Thus, the neural signal predominantly reflects the accumulated evidence.

The neural response to the input evidence elements increases over time and peaks at 133 ms following a click. That time approximately coincides with an increase in the encoding of the cumulated decision evidence. This suggests that the neural effect of the cumulated evidence is most prominent shortly after a click is registered in the neural signal.

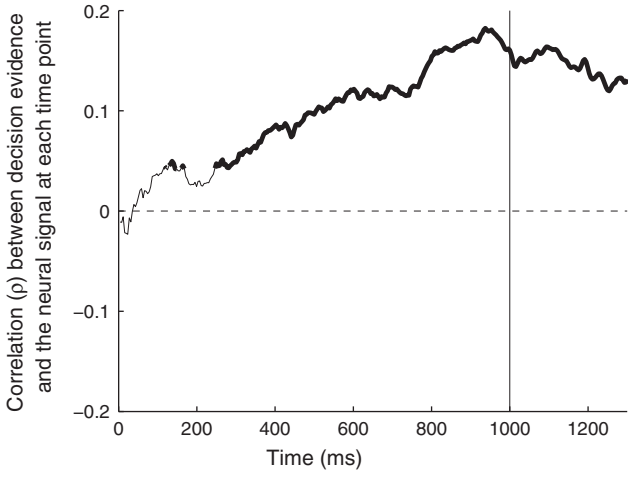

Fig. 7. The neural signal encodes the instantaneous value of decision evidence during evidence integration. Correlation (ρ) of the neural signal and the decision variable at each time point during the stimulus period (starting at 0 ms and ending at 1000 ms), for all trials that result in a button press. The thick segments give the time points at which the correlation is significant ($p < 0.05$). When computing the correlation, the neural signal has been shifted in time by 74 ms to account for the lag of the neural signal behind decision evidence (74 ms (Fig. 6); a particular value of the lag does not substantially change the result).

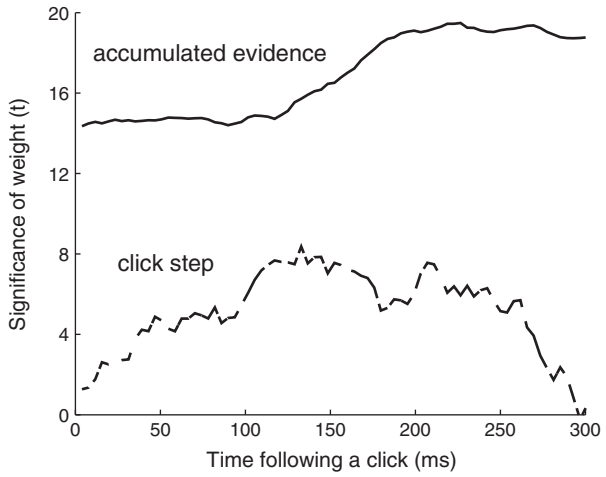

Fig. 8. Comparison of the encoding of the input quanta and the cumulated evidence. The figure gives the *t*-statistic associated with the weights in a linear model in which the instantaneous cumulated evidence (solid) and a signal that represents the onset and the polarity of each click (dashed; see text) is regressed on the neural signal. The regression is performed separately at each time point following a click, for every click, and for all button press choices.

Whole-brain analysis of the representation of the decision variable

Our data indicate that the left centroparietal regions encode, besides a decision outcome, also the input decision variable. We next performed a whole-brain analysis to investigate whether the decision variable is represented in any other cortical region. To do so, we quantified the neural effect of decision evidence for each channel by fitting a line to the relationship between neural desynchronization during the delay period and decision evidence, and determining whether the slope of this line is significantly different from zero. The associated *p*-values, corrected for multiple comparisons, are given in Fig. 9. The left panel in this figure shows that the human cortex encodes decision evidence for saccadic choices. The effect for saccadic choices peaks over parietal channels P4 ($p < 10^{-8}$, $F_{1,1713} = 36.8$, ANCOVA) and Pz ($p < 10^{-5}$, $F_{1,1713} = 19.7$). The bias toward the right hemisphere is expected given that subjects made each saccade to a target located in the left visual hemifield (Hamed et al., 2001; Medendorp et al., 2007). In comparison, the neural effect of decision evidence for button press choices (right panel) peaks in contralateral centroparietal regions, in particular, over channels C3 ($p < 10^{-7}$, $F_{1,2182} = 32.3$) and CP3 ($p < 10^{-8}$, $F_{1,2182} = 36.9$). The effect of decision evidence for button press choices is also observed, to a somewhat reduced extent, in centroparietal regions of the ipsilateral hemisphere.

In an additional analysis, we investigated the dynamics of the decision process in the right parietal cortex (channels P4 and Pz, Fig. 10). This region shows dynamics similar to those observed over the contralateral centroparietal cortex (Fig. 2C). This analysis reveals that in comparison to the left centroparietal cortex, the right parietal cortex encodes decision evidence for both movement types.

Representation of the decision variable at each frequency

We investigated how the effect of decision evidence is represented at each individual frequency of the neural signals. To do so, we computed the effect of decision evidence for each frequency in the range 1 Hz to 50 Hz (Fig. 11). The figure reveals that the effect is consistently significant in the frequency band from about 8 Hz to about 22 Hz. Starting at about 30 Hz, the effect reverses its sign and becomes non-significant. This result is consistent with previous studies that observe an effect sign reversal in high-frequency compared to low-frequency bands (Crone et al., 1998b; Donner et al., 2009; Pfurtscheller et al., 2003). Although in our hands the decision-related effect for higher frequencies is non-significant, there is some evidence that high-frequency (gamma) oscillations carry choice-predictive information (Donner et al., 2009). This high-frequency signal may possibly encode also a decision variable. Future studies using more sensitive imaging modalities (e.g., electrocorticography (ECoG), magnetoencephalography (MEG)) should investigate this issue.

Control for reaction time, eye gaze, and sensory signals

Finally, we tested whether the observed effect of decision evidence could be explained by other factors, including the subject's reaction time, the mean and variance in eye gaze, and sensory signals of the hand. To account for these factors, we included, besides decision evidence, also the subject's reaction time and eye gaze mean position and variance as additional regressors on neural activity (see Eq. (3)). We computed the kinematic parameters of eye gaze both during the delay interval, and during movement. These additional factors did not significantly change the effects of decision evidence when these factors were considered in either the delay interval (modulation of desynchronization at C3 and CP3 during delay period by decision evidence (slope) for button presses: 37.4%; slope for saccades: 3.3%) or during movement (slope for button presses: 38.5%; slope for saccades: 3.3%). We also tested whether the decision-related signal in centroparietal regions could reflect sensory input related to a change of activation of the hand muscles.

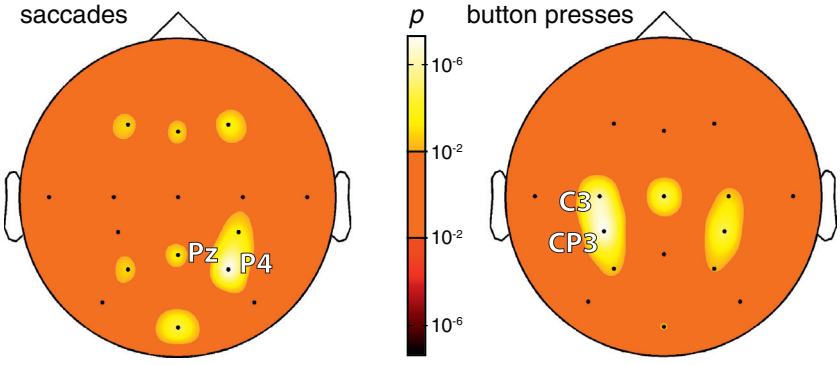

Fig. 9. Whole-brain analysis of the representation of decision evidence. The significance of the effect of decision evidence is rendered in color for each channel, separately for saccade choices (left) and button press choices (right). The bright (dark) hues of the color bar indicate cases for which the effects are positive (negative), that is, where stronger evidence is significantly associated with more (less) desynchronization. For both saccades (left) and button presses (right), the effect is not negative for any channel. For saccades, the effect of decision evidence is strongest at parietal channels P4 and Pz. For button presses, the effect is strongest at motor channels CP3. The significance values are corrected for the number of channels (i.e., 16) and for the number of observations (i.e., 2)—by a factor of 32.

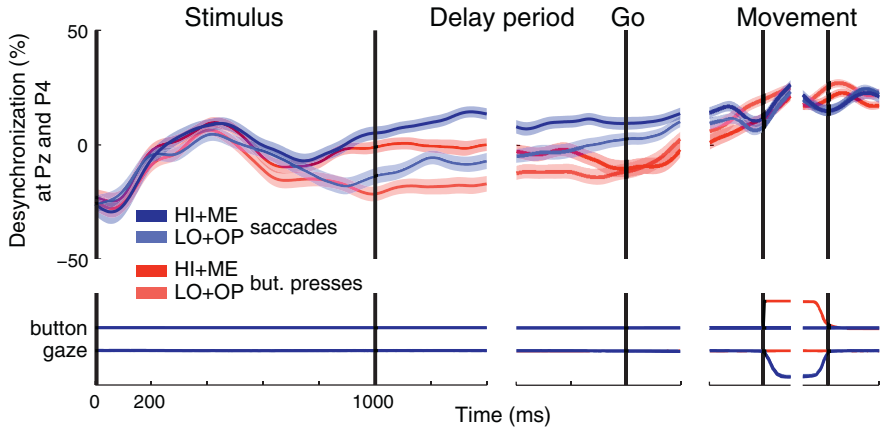

Fig. 10. Dynamics of the low-frequency neural signal in the right parietal cortex. Same format as in Fig. 2C. Activity was averaged over channels P4 and Pz.

A different set of subjects performed a modified version of the task (see the Materials and methods section) while we recorded electromyographic (EMG) activity of the flexor carpi radialis and flexor digitorum superficialis muscles in addition to EEG signals. The activity of the more sensitive flexor carpi radialis muscle was minimal during the stimulus period, and the first time sample of the muscle activity that distinguishes between the two choices occurs at 660 ms following stimulus onset (Wilcoxon rank sum test, $p < 0.001$, see the Materials and methods section). The activity of the hand muscle is notable first shortly before subjects make the hand movement. In comparison, the signal in the centroparietal cortex, extracted in the same way as in the present study, begins to significantly distinguish between the two choices already at 230 ms (Wilcoxon rank sum test, $p < 0.001$) following stimulus onset. Thus, the activation of the muscle substantially lags behind the activation of the cortex. Hence, it is unlikely that the effects identified in our study are due to sensory activation.

Discussion

We tested whether a low-frequency neural signal recorded over the centroparietal cortex and reported previously to reflect the choice of a hand movement (Donner et al., 2009) is modulated by the decision variable informing the choice of a hand movement. We found that the signal strongly encodes the decision variable on which subjects base the decision to make a hand movement. On each trial, the signal ramps up with a rate that is strongly graded with the DV, remains at a steady level during the delay period, peaks shortly before a hand movement, and falls off upon the termination of the movement. We further found that the signal show properties of evidence accumulation. In particular, the signal encodes each quantum of evidence in a ramp-like fashion and distinguishes the quantum supporting from the quantum contradicting the decision to choose a button press.

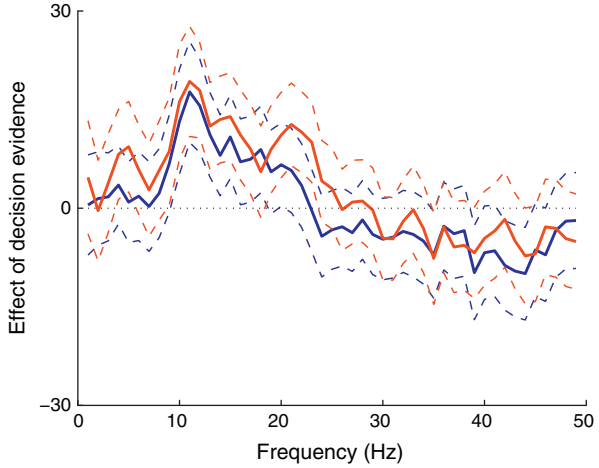

Fig. 11. Cortical representation of decision evidence as a function of frequency of neural signals. The effect of decision evidence (slope) outlined by its 95% confidence intervals as a function of frequency, separately for button press (red) and saccade (blue) choices. The signals at each frequency were measured in the delay interval and the effects were averaged over all channels.

Studies of decision-related neural dynamics in non-human primates have been subjected to the criticism that decision variables are encoded in oculomotor circuits (Gold and Shadlen, 2000, 2002; Horwitz and Newsome, 1999; Kable and Glimcher, 2009; Platt and Glimcher, 1999) simply because animals were conditioned to map perceptual decisions onto motor outputs through extensive training (Connolly et al., 2009). Our finding argues against this lingering criticism by showing that a perceptual decision variable is represented in motor circuits of the brain even when subjects are not extensively trained in a decision task.

The presence of a DV in the somatomotor system has been demonstrated in a recent study (Selen et al., 2012). In this study, human subjects decided on the direction of a dot motion stimulus and communicated their decision using an arm movement. The authors found that when the muscular system is perturbed to elicit a spinal cord reflex, the electromyographic (EMG) activity of the arm muscles reveals the current state of the DV at the time of the perturbation. Thus, the spinal cord reflex gates the developing perceptual DV into the muscles, presumably from an upstream cortical region. Here we show that the cortex indeed encodes a developing DV for hand movement choices. Furthermore, the approach of recording cortical signals allows us to characterize the dynamics of the decision-related effects not only at a time following a perturbation but continuously throughout the decision process and at the time of the behavioral response (Kubanek and Kaplan, 2012).

The model we used to describe the behavior of subjects in our task is an extension of the drift-diffusion model (DDM), a model commonly applied to explain choice behavior and reaction time in reaction time decision tasks (Edwards, 1965; Gold and Shadlen, 2007; Ratcliff and McKoon, 2008; Stone, 1960; Vickers, 1970). In a simple, symmetric, and noiseless DDM, in which each pro-quantum of evidence contributes a change in the decision variable δ and each contra-quantum to a change of $-\delta$, the value of the decision variable at the end of the stimulus period is $C_r\delta - C_l\delta = (C_r - C_l)\delta$, where C_r is the number of cumulated quanta in favor of and C_l against a decision. Our model features the same principal term $(C_r - C_l)$ and extends this term in two ways to accommodate the variable delay incorporated in our task. First and importantly, in reaction time tasks assumed by the DDM, subjects make a choice at the time they have reached a decision. In contrast, in our task, subjects are forced, after a delay, to make a choice regardless of

the current amount of cumulated evidence. In our model, this enforced commitment to a choice alternative is modeled using a sigmoid function that rectifies the difference in the two accumulators. Second and less importantly, we included in the model a normalizing term ($C_r + C_l$) for the overall number of evidence elements presented on a given trial.

The low-frequency neural signal recorded over centro-parietal regions in our study shows two critical properties of the diffusion-to-bound class of behavioral models (Edwards, 1965; Gold and Shadlen, 2007; Ratcliff and McKoon, 2008; Stone, 1960; Vickers, 1970). First, the signal encodes the amount of evidence that has cumulated for a button press during the stimulus period (Figs. 3 and 4). Moreover, the signal shows properties of integration of each individual piece of evidence (Fig. 6). In particular, the signal, shortly after a click is presented, distinguishes a pro-button piece of evidence (a click in the right ear) from a contra-button piece of evidence (a click in the left ear; Fig. 6). Furthermore, this response to each piece of evidence appears to be integrated over time as the effect retains the level it has reached following the response to each piece of evidence. The signal shows these properties already early during the stimulus period, for clicks occurring within the first 400 ms. Second, the signal reaches a common level at the time of the button press (Fig. 3), regardless of the amount of evidence that a subject has obtained for the decision to make a button press. The hypothesis that choice is made when a signal representing cumulated evidence reaches a critical level (Edwards, 1965; Ratcliff and McKoon, 2008; Stone, 1960; Vickers, 1970) has found initial support through neural data in the macaque oculomotor system (see Gold and Shadlen, 2007 for an overview of that literature). Our study and a recent study (O'Connell et al., 2012) suggest that low-frequency signals recorded over centroparietal regions may also exhibit this property. These two properties of the neural signal reported here encourage future studies to use a reaction-time tasks (e.g., subject responds at the time she has reached a decision) to investigate the early evidence accumulation process under the behavioral proxy of the drift-diffusion model.

The modulation of neural signals recorded in humans by a decision variable has in part been investigated by three recent studies (Donner et al., 2009; O'Connell et al., 2012; Wyart et al., 2012). The individual studies share some common aspects but differ in important ways, which are discussed below.

In regard to encoding a DV, an MEG study (Donner et al., 2009) found that an integral of gamma activity over a putative human homologue of macaque area MT correlates with signals recorded over centroparietal regions. Although this finding suggests that centroparietal signals may encode a DV (the integral of motion-sensitive activity in MT), this study does not *directly test* whether centroparietal regions encode the DV on which subjects base their decision in that task (i.e., the DV inferred from subjects' choice behavior). For instance, an integral of gamma activity in brain regions other than the MT homologue may also correlate with the centroparietal signals. This would not necessarily imply that centroparietal signals represent a DV. We directly tested this hypothesis by inferring the DV on which subjects base their decision and by sorting the neural signal based on the DV. We support the hypothesis raised by the work of Donner et al. (2009) by showing a prominent grading of the neural signals by the inferred DV.

The neural signal reported in our study encodes the sign of each element of incoming decision evidence. A recent study (Wyart et al., 2012) also found that a low-frequency signal recorded over centroparietal regions encodes the individual elements of decision evidence, in particular the orientation of each successive visual patch (their Fig. 7A). However, in that study, the signal starts to significantly encode the orientation of each decision element first at about 400 ms following an element onset (their Fig. 7A). This is substantially later compared to our study, in which we observe significant encoding as early as at 74 ms following an element onset. The delay of the response in that study compared to our rapid response may be due to the relatively longer time required to assess the direction of each decision element compared to the side of the occurrence of simple click sounds used in our study.

Our study and the study of Wyart et al. (2012) show an additional important difference in regard to the encoding of the cumulative sum of the evidence elements (the DV). In our study, the neural signal significantly encodes the DV already at 211 ms (137 + 74 ms) following the stimulus onset (Fig. 7). This is 789 ms (the time until the rest of the stimulus period) plus 800 ms (the average duration of the delay period) plus 492 ms (the average reaction time), together 2081 ms prior to a button press. In comparison, in the study of Wyart et al. (2012), the signal encodes the DV in that task—the sum of the orientations of the individual elements—earliest at about 500 ms preceding movement onset (their Supplementary Fig. 7A). This is a surprising result given that the signal in our study and the signals recorded in the oculomotor system of the monkey encode the decision variable early in the trial, when subjects assess the decision evidence (e.g., Gold and Shadlen, 2007; Platt and Glimcher, 1999). Progressively through the trial, once a decision is made, the grading of the signals due to decision evidence vanishes and is replaced with a signal that indicates subjects' choice (Gold and Shadlen, 2007; Platt and Glimcher, 1999). Neither a study working with a low-frequency centroparietal signal similar to that used in our study (O'Connell et al., 2012) has found a pre-movement grading of the signal due to decision-related response parameters. It is possible that the additional signal processing step used in the study of Wyart et al. (2012)—the subtraction of the signal of one hemisphere from the signal over the other hemisphere—can explain the discrepancy between the studies. Another and perhaps more likely possibility is that the discrepancy is due to the different way of reporting a decision (left versus right hand in Wyart et al., 2012, a hand versus no hand (eye) response in our study; see a paragraph dedicated to this issue below in the Discussion section).

A recent study (O'Connell et al., 2012) in part investigated the beta band responses (a portion of the wider low-frequency range used in our study) in a detection task. The study found a significant modulation of the beta activity over centroparietal regions by the reaction time (their Fig. 1C middle; see also the same effect in Tzagarakis et al., 2010), the variable regressed out as a confounding variable in our study. Notably, the signal in the detection task of O'Connell et al. (2012) is not modulated by the properties of the stimulus (stimulus contrast, their Fig. 2C top). In contrast, in our task, low-frequency rhythms over centroparietal regions are prominently modulated by a decision variable, even when the reaction time is accounted for. The difference in the results may reflect the difference in the tasks (e.g., a delay-period task here, a reaction-time task in O'Connell et al., 2012).

A previous study (Donner et al., 2009) reports a low-frequency signal recorded over centroparietal regions that builds up gradually to indicate a subject's choice of a hand movement. This effect has been proposed to reflect the suppression of intrinsic oscillatory activity during motor preparation (Crone et al., 1998a; Donner et al., 2009; Pfurtscheller and Lopes da Silva, 1999). We found that in addition to this effect, the low-frequency signal is strongly modulated by a cognitive, perceptual decision variable, and encodes with a short latency the polarity of each quantum of the sensory evidence. This suggests that the low-frequency signal reflects a juxtaposition of movement-related, planning processes and cognitive, decision-related processes. The decision-related modulation reported in our study is prominent, prompting a thorough investigation of the mechanism that gives rise to the low-frequency signal reported in this and previous studies (Donner et al., 2009; Neuper et al., 2006; Pfurtscheller and Lopes da Silva, 1999). In this regard, it has been proposed that cortical signals in the low-frequency range reflect cortico–striato–thalamo–cortical interactions (Lopes da Silva, 1991; Steriade and Llinás, 1988). In particular, it has been found that the magnitude of desynchronization of low-frequency cortical signals is a robust correlate of cellular excitability in thalamo–cortical circuits (Pfurtscheller et al., 1996; Steriade and Llinás, 1988). Moreover, it has been proposed that the thalamo–cortical interaction acts as a cognitive gate that gives rise to a desired movement and inhibits other movement alternatives (Leblois et al., 2006; Lopes da Silva, 1991; Mink, 1996). At

the circuit level (Jensen et al., 2005), increased neural synchrony in the low-frequency range has been associated with increased inhibition of neural circuitry and decreased synchrony (i.e., asynchrony) with disinhibition of neural circuitry. This model fits the neural effect observed in our and previous studies (Donner et al., 2009; Neuper et al., 2006; Pfurtscheller and Lopes da Silva, 1999), in which centroparietal activity becomes increasingly desynchronized the closer a subject approaches an act. At the same time, while our data are consistent with the body of literature on the functional significance of low-frequency oscillations, the specific origin and mechanism of the decision-related signal identified in this study remains to be explored. Although it would be possible to sample the centroparietal signal at higher spatial density, inferring the spatial origin from EEG signals is a complex and indirect process of unclear reliability. Furthermore, EEG does not readily provide access to signals at higher frequencies, in particular signals in the gamma band (>40 Hz; Donner et al., 2009), which likely index activation of local populations of neurons rather than interactions between subcortical and cortical structures. Thus, to fully elucidate the mechanism underlying the prominent decision-related signal identified in this study, future studies could record field potentials in human or non-human primates, which provide ready access to both the low-frequency and the high-frequency ranges of neural activity, and can also accurately locate the origin of the signal source.

We have shown that a low-frequency oscillatory signal recorded over the centroparietal cortex in humans encodes a developing decision variable. Future studies featuring high spatial resolution could investigate whether the effect can be decomposed into possibly independent features in particular frequency bands and in particular regions. Future studies may further test whether signals of different kinds, e.g., cortical potentials (O'Connell et al., 2012; Schurger et al., 2012), encode the dynamics of a developing decision variable in decision tasks.

An important attribute of our task is that subjects responded with one hand. This is critical, as Fig. 9 (right) reveals that for button press choices, decision evidence is represented not only over contralateral centroparietal regions but also over regions ipsilateral to the responding hand. In light of this finding, if subjects decided between a left-hand and a right-hand button press (e.g., Donner et al., 2009; Wyart et al., 2012), the signals underlying the decision which hand to choose would engage both hemispheres. This could result in a poor specificity of the signal informing a given choice, and, as a consequence, the prominent effect of decision evidence shown in our study may not be detectable in such tasks.

In our task, we did not test asymmetries in the engagement of motor structures—subject always responded using the right hand or a saccade to a left target. However, other studies (e.g., Donner et al., 2009) suggest that the neural responses that encode the plan to make a movement with a right versus a left hand are fairly counter-balanced (Fig. 2C in Donner et al., 2009). The figure shows that when a right hand movement is planned, the left hemisphere shows a low-frequency desynchronization; whereas when a left hand movement is planned, it is the right hemisphere that is desynchronized. Although (Donner et al., 2009) do not directly test the effect of a DV, our data (our Fig. 9, button presses) suggest that the effect of the DV is also lateralized. The effect of the DV during plans to make an eye movement also appears to be lateralized (our Fig. 9, saccades), in particular over parietal–occipital regions. The study by (Medendorp et al., 2007) suggests that had subjects in our study planned an eye movement to a right target (instead of to a left target), we would see a stronger activation of the hemisphere opposite to the currently activated one. These findings suggest that our results may be extensible to the case in which subjects are asked to respond with a reversed response contingency (button press with the left hand, saccade to the right target).

Our findings contribute to the current debate whether cognitive processes function separately from or are closely tied to the function of motor systems (Anderson, 2003; Brooks, 1991; Clark, 1999; Ghazanfar and Turesson, 2008; Markman and Dietrich, 2000; Wilson, 2002). In our task, subjects respond with one of two different movement types—a button press or a saccade. This design allows us to test whether the decision-related signal recorded over the centroparietal cortex is related to a generic cognitive process (Maunsell, 2004)—such as, attention (Gottlieb, 2007; Peck et al., 2009), reward expectation (Kable and Glimcher, 2009), motivation (Roesch and Olson, 2004), or task difficulty (Chen et al., 2008)—or whether the signal is instead more closely tied to a particular action. We found that the effect of decision evidence is observed over centroparietal regions specifically for hand movement choices (Fig. 2B); the effect is not present during trials that resulted in a saccade. This result is further supported by a recent finding (O'Connell et al., 2012) that shows a modulation of a low-frequency signal over the centroparietal cortex by RT specifically when subjects plan a response using a hand movement. The effect is not observed when the response is withheld. This suggests that the representation of decision evidence in centroparietal regions reflects the degree of commitment to select a somatomotor action or a degree of motor preparation (Bestmann et al., 2008). These findings imply that decision-making and action planning do not necessarily occur sequentially and within functionally separate modules (Gottlieb, 2007; Schall, 2002; Tversky and Kahneman, 1981); these two processes can be closely intertwined.

In summary, we found that a low-frequency electrophysiological signal recorded over the centroparietal cortex is strongly modulated by the variable on which subjects based their decision to make a hand movement. Thus, decision-related signals are represented within the same somatomotor circuits that represent the command to make a hand movement. This observation extends the analogous finding made in monkey oculomotor circuits for eye movement choices to somatomotor circuits of humans for hand movement choices. We further found that the signal reported in our study shows a defining property of the diffusion-to-bound class of models—the accumulation of evidence over time. In addition, this signal seems to show a second defining property of the diffusion-to-bound models—the integration to a bound—as the signal reaches a common, evidence-independent level shortly before a movement. A similar observation has recently been made by O'Connell et al. (2012). This property should be tested in reaction-time tasks in the future. The finding that a neural signal recorded in humans is modulated by a cognitive, decision-related variable may open future door to the investigation of the dynamics of decision-related processes associated with a behavioral response in humans.

Acknowledgments

We thank Peter Brunner for the discussions on the task. We thank Griffin Milsap, Jeremy Hill, Bill Sarnacki, and Peter Brunner for their technical assistance with data collection. This study was supported by grants from the NIH (EY012135 (LHS), EY002687 (LHS), EB006356 (GS), EB000856 (GS)) and the US Army Research Office (W911NF-08-1-0216 (GS), W911NF-07-1-0415 (GS), W911NF-12-1-0109 (GS)).

Conflict of interest statement

The authors declare no conflict of interests.

References

Anderson, M.L., 2003. Embodied cognition: a field guide. Artif. Intell. 149, 91–130.
Bestmann, S., Swayne, O., Blankenburg, F., Ruff, C., Haggard, P., Weiskopf, N., Josephs, O., Driver, J., Rothwell, J., Ward, N., 2008. Dorsal premotor cortex exerts state-dependent causal influences on activity in contralateral primary motor and dorsal premotor cortex. Cereb. Cortex 18, 1281–1291.
Britten, K.H., Shadlen, M.N., Newsome, W.T., Movshon, J.A., 1992. The analysis of visual motion: a comparison of neuronal and psychophysical performance. J. Neurosci. 12, 4745–4765.
Brooks, R., 1991. Intelligence without representation. Artif. Intell. 47, 139–159.
Brunton, B.W., Botvinick, M.M., Brody, C.D., 2013. Rats and humans can optimally accumulate evidence for decision-making. Science 340, 95–98.
Chen, Y., Martinez-Conde, S., Macknik, S., Bereshpolova, Y., Swadlow, H., Alonso, J., 2008. Task difficulty modulates the activity of specific neuronal populations in primary visual cortex. Nat. Neurosci. 11, 974–982.

Clark, A., 1999. An embodied cognitive science? Trends Cogn. Sci. 3, 345–351.
Connolly, P., Bennur, S., Gold, J., 2009. Correlates of perceptual learning in an oculomotor decision variable. J. Neurosci. 29, 2136–2150.
Crone, N., Miglioretti, D., Gordon, B., Sieracki, J., Wilson, M., Uematsu, S., Lesser, R., 1998a. Functional mapping of human sensorimotor cortex with electrocorticographic spectral analysis. I. alpha and beta event-related desynchronization. Brain 121, 2271–2299.
Crone, N.E., Miglioretti, D.L., Gordon, B., Lesser, R.P., 1998b. Functional mapping of human sensorimotor cortex with electrocorticographic spectral analysis. II. event-related synchronization in the gamma band. Brain 121 (Pt 12), 2301–2315.
Donner, T.H., Siegel, M., Fries, P., Engel, A.K., 2009. Buildup of choice-predictive activity in human motor cortex during perceptual decision making. Curr. Biol. 19, 1581–1585.
Edwards, W., 1965. Optimal strategies for seeking information: models for statistics, choice reaction times, and human information processing. J. Math. Psychol. 2, 312–329.
Ghazanfar, A.A., Turesson, H.K., 2008. How robots will teach us how the brain works. Nat. Neurosci. 11, 3.
Gold, J., Shadlen, M., 2000. Representation of a perceptual decision in developing oculomotor commands. Nature 404, 390–394.
Gold, J.I., Shadlen, M.N., 2002. Banburismus and the brain: decoding the relationship between sensory stimuli, decisions, and reward. Neuron 36, 299–308.
Gold, J.I., Shadlen, M.N., 2007. The neural basis of decision making. Annu. Rev. Neurosci. 30, 535–574.
Gottlieb, J., 2007. From thought to action: the parietal cortex as a bridge between perception, action, and cognition. Neuron 53, 9–16.
Haegens, S., Nácher, V., Hernández, A., Luna, R., Jensen, O., Romo, R., 2011. Beta oscillations in the monkey sensorimotor network reflect somatosensory decision making. Proc. Natl. Acad. Sci. U. S. A. 108, 10708–10713.
Hamed, S.B., Duhamel, J.R., Bremmer, F., Graf, W., 2001. Representation of the visual field in the lateral intraparietal area of macaque monkeys: a quantitative receptive field analysis. Exp. Brain Res. 140, 127–144.
Hanks, T., Ditterich, J., Shadlen, M., 2006. Microstimulation of macaque area lip affects decision-making in a motion discrimination task. Nat. Neurosci. 9, 682–689.
Hernández, A., Nácher, V., Luna, R., Zainos, A., Lemus, L., Alvarez, M., Vázquez, Y., Camarillo, L., Romo, R., 2010. Decoding a perceptual decision process across cortex. Neuron 66, 300–314.
Horwitz, G., Newsome, W., 1999. Separate signals for target selection and movement specification in the superior colliculus. Science 284, 1158–1161.
Jensen, O., Goel, P., Kopell, N., Pohja, M., Hari, R., Ermentrout, B., 2005. On the human sensorimotor-cortex beta rhythm: sources and modeling. NeuroImage 26, 347–355.
Kable, J.W., Glimcher, P.W., 2009. The neurobiology of decision: consensus and controversy. Neuron 63, 733–745.
Kubanek, J., Kaplan, D., 2012. Evidence for a decision variable in the human motor system. J. Neurosci. 32, 8110–8111.
Leblois, A., Boraud, T., Meissner, W., Bergman, H., Hansel, D., 2006. Competition between feedback loops underlies normal and pathological dynamics in the basal ganglia. J. Neurosci. 26, 3567–3583.
Lopes da Silva, F., 1991. Neural mechanisms underlying brain waves: from neural membranes to networks. Electroencephalogr. Clin. Neurophysiol. 79, 81–93.
Markman, A., Dietrich, E., 2000. Extending the classical view of representation. Trends Cogn. Sci. 4, 470–475.
Maunsell, J.H.R., 2004. Neuronal representations of cognitive state: reward or attention? Trends Cogn. Sci. 8, 261–265.
Medendorp, W.P., Kramer, G.F.I., Jensen, O., Oostenveld, R., Schoffelen, J.M., Fries, P., 2007. Oscillatory activity in human parietal and occipital cortex shows hemispheric lateralization and memory effects in a delayed double-step saccade task. Cereb. Cortex 17, 2364–2374.
Mink, J., 1996. The basal ganglia: focused selection and inhibition of competing motor programs. Prog. Neurobiol. 50, 381–425.
Moyer, R., Bayer, R., 1976. Mental comparison and the symbolic distance effect. Cogn. Psychol. 8, 228–246.
Neuper, C., Wörtz, M., Pfurtscheller, G., 2006. ERD/ERS patterns reflecting sensorimotor activation and deactivation. Prog. Brain Res. 159, 211–222.
O'Connell, R.G., Dockree, P.M., Kelly, S.P., 2012. A supramodal accumulation-to-bound signal that determines perceptual decisions in humans. Nat. Neurosci. 15, 1729–1735.
Peck, C.J., Jangraw, D.C., Suzuki, M., Efem, R., Gottlieb, J., 2009. Reward modulates attention independently of action value in posterior parietal cortex. J. Neurosci. 29, 11182–11191.
Pfurtscheller, G., Lopes da Silva, F., 1999. Event-related EEG/MEG synchronization and desynchronization: basic principles. Clin. Neurophysiol. 110, 1842–1857.
Pfurtscheller, G., Stancak, A., Neuper, C., 1996. Event-related synchronization (ERS) in the alpha band—an electrophysiological correlate of cortical idling: a review. Int. J. Psychophysiol. 24, 39–46.
Pfurtscheller, G., Graimann, B., Huggins, J.E., Levine, S.P., Schuh, L.A., 2003. Spatiotemporal patterns of beta desynchronization and gamma synchronization in corticographic data during self-paced movement. Clin. Neurophysiol. 114, 1226–1236.
Platt, M., Glimcher, P., 1999. Neural correlates of decision variables in parietal cortex. Nature 400, 233–238.
Raftery, A.E., 1995. Bayesian model selection in social research. Sociol. Methodol. 25, 111–164.
Ratcliff, R., McKoon, G., 2008. The diffusion decision model: theory and data for two-choice decision tasks. Neural Comput. 20, 873–922.
Roesch, M.R., Olson, C.R., 2004. Neuronal activity related to reward value and motivation in primate frontal cortex. Science 304, 307–310.
Roitman, J.D., Shadlen, M.N., 2002. Response of neurons in the lateral intraparietal area during a combined visual discrimination reaction time task. J. Neurosci. 22, 9475–9489.
Schalk, G., Mellinger, J., 2010. A Practical Guide to Brain-computer Interfacing with BCI2000, 1st edition. Springer, London, UK.
Schalk, G., McFarland, D., Hinterberger, T., Birbaumer, N., Wolpaw, J., 2004. BCI 2000: a general-purpose brain-computer interface (BCI) system. IEEE Trans. Biomed. Eng. 51, 1034–1043.
Schall, J.D., 2002. The neural selection and control of saccades by the frontal eye field. Philos. Trans. R. Soc. Lond. B Biol. Sci. 357, 1073–1082.
Schurger, A., Sitt, J.D., Dehaene, S., 2012. An accumulator model for spontaneous neural activity prior to self-initiated movement. Proc. Natl. Acad. Sci. 109 (42), E2904–E2913.
Schwarz, G., 1978. Estimating the dimension of a model. Ann. Stat. 6, 461–464.
Selen, L., Shadlen, M., Wolpert, D., 2012. Deliberation in the motor system: reflex gains track evolving evidence leading to a decision. J. Neurosci. 32, 2276–2286.
Shadlen, M., Newsome, W., 1996. Motion perception: seeing and deciding. Proc. Natl. Acad. Sci. 93, 628.
Steriade, M., Llinás, R., 1988. The functional states of the thalamus and the associated neuronal interplay. Physiol. Rev. 68, 649–742.
Stone, M., 1960. Models for choice-reaction time. Psychometrika 25, 251–260.
Tversky, A., Kahneman, D., 1981. The framing of decisions and the psychology of choice. Science 211, 453–458.
Tzagarakis, C., Ince, N.F., Leuthold, A.C., Pellizzer, G., 2010. Beta-band activity during motor planning reflects response uncertainty. J. Neurosci. 30, 11270–11277.
Vickers, D., 1970. Evidence for an accumulator model of psychophysical discrimination. Ergonomics 13, 37–58.
Wilson, M., 2002. Six views of embodied cognition. Psychon. Bull. Rev. 9, 625–636.
Wyart, V., de Gardelle, V., Scholl, J., Summerfield, C., 2012. Rhythmic fluctuations in evidence accumulation during decision making in the human brain. Neuron 76, 847–858.